

Free Space Optical Communication: Review Paper

J.A. Akinwumi¹, J.O. Bandele¹

¹Department of Electrical, Electronics and Computer Engineering, College of Engineering, Afe Babalola University, Ado-Ekiti, Ekiti State, Nigeria, P.M.B 5454
Corresponding Author: J.A. Akinwumi

ABSTRACT: Free-space optical communication systems have received significant attention from researchers in recent years. In this paper, we review previous work on mitigating scintillation effects of atmospheric turbulence on Free Space Optical communication systems. Techniques reviewed include: equalization in semiconductor optical amplifier, spatial and temporal diversity, aperture averaging, and coding schemes. We discuss various free space optical communication system and channel models, relay-assisted systems and far-field assumptions. **KEYWORDS-** Free space optical communication, spatial diversity, coding schemes, signal equalization

Date of Submission: 28-09-2018

Date of acceptance: 08-10-2018

I. Introduction

Free space optical (FSO) communication is a candidate solution for low-cost, license-free, rapidly-deployable and high capacity links. FSO systems are used in indoor wireless local area networks, interconnection of network nodes, metropolitan area networks and rapidly deployable communications system in disaster recovery situations. FSO systems use either lasers or light emitting diodes (LED) to transmit a modulated beam of visible or infrared light. Optical transmission must subscribe to safety standards for potential eye damage. The use of infrared wavelengths such as 1.55 μ m is advantageous because eye hazards are less problematic [8]. FSO systems are secured against eavesdropping and jamming due to their directional and narrow beams. They can be used in applications including last-mile access, High-Definition Television (HDTV) transmission, fiber back-up and back-haul for wireless cellular networks.

However, atmospheric turbulence results in time-varying changes in the refractive-index which further results in time-varying power fluctuations noticeable over distances of 1km or longer. Under intense turbulence, the received signal decreases below the receiver sensitivity and the link is lost [3]. This is described as fading or scintillation and it affects both the capacity and latency of optical wireless systems. A number of techniques for overcoming fading include: coding schemes, spatial and temporal diversity, aperture averaging and signal equalization in semiconductor optical amplifier (SOA).

In Section 2 of this paper, we review previous work discussing the different techniques for mitigating scintillation as a result of atmospheric turbulence. The techniques include: equalization in semiconductor optical amplifiers [1-3], spatial diversity [4-9][17][22][25][27-30], aperture averaging [23-24] and coding schemes [32-34]. We discuss the system and channel models for free space optical communication system, relay-assisted systems [18-20] and far-field assumptions [21] in Section 3. We conclude the paper in Section 4.

II. Techniques For Mitigating Turbulence-induced Scintillation

Atmospheric turbulence is a major challenge for free space optical communication systems especially over distances of 1 km or longer. We discuss various techniques for mitigating the scintillation effects of atmospheric turbulence on free space optical communication systems.

2.1 Signal Equalization in Semiconductor Optical Amplifier

The SOA or Erbium Doped Optical Amplifier (EDFA) can reduce intensity fluctuations and amplify the optical signal when it is gain saturated by the input turbulent signal. It has been applied to suppress cross-talk and intensity noise in wavelength-division-multiplexing systems. Previous work implemented receiver structures and the bit error rate (BER) and signal-to-noise ratio performance of each receiver is measured and compared for various turbulence levels. Three different turbulence scenarios A, B and C were created in the laboratory environment using a turbulence box (30 cm wide, 61 cm long, and 26 cm height) with four electric heating elements and five small fans [1]. Five receiver structures were implemented using techniques such as fiberless direct detection (DD), fiber-coupled (FC) detection without optical amplification, fiber-coupled detection using SOA in amplification mode and conversion mode (CSOA), and fiber-coupled detection using Erbium Doped Optical Amplifier (EDFA).

The experimental setup is as shown in figure 1. A continuous wave (CW) laser operating at 1550nm is modulated by a pseudorandom binary sequence operating at 1.244 Gb/s and amplified by an EDFA. The input optical power at the receiver is controlled using a tunable optical attenuator before free space propagation. The focal length of the imaging lens is 7.5cm while the diameter is 2.5cm. This creates a convergent optical beam. The turbulence box is positioned between the lens and the focus point. The box length is the same as the optical path length. Except for DD, a 4-mm diameter collimating lens is used to couple light into a fiber in all other receiver structures. The detected signal is compared to the original signal for BER measurements.

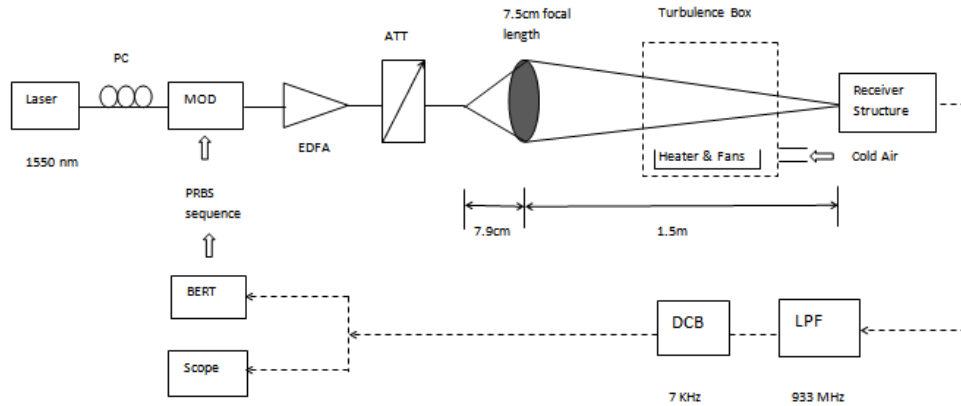


Figure 1: The schematic diagram of experimental setup. The optical connections are shown by solid lines while dashed lines show electrical connections. MOD: intensity modulator; EDFA: erbium-doped fiber amplifier; ATT: tunable optical attenuator; PC: polarization controller; PD: photodiode; DCB: DC block; BERT: BER tester; LPF: Low Pass Filter

In the case of weak turbulence, performance degradation of FSO system is very high. As a result, there is need to eliminate or suppress the effects of turbulence-induced scintillation. Under turbulence level A with low scintillation noise, a saturated optical amplifier or EDFA can eliminate almost all the scintillation noise. It is not possible to remove the scintillation noise completely under higher turbulence level B and C. The EDFA provides higher improvement. No data transmission can be achieved using only DD or FC receiver structures at turbulence level C. In all three levels of turbulence (A, B, C), the EDFA provides better BER performance than the SOA. The improvement in system performance is due to two phenomena: gain squeezing and the increasing receiver sensitivity by amplification.

In medium-to-strong turbulence governed by Gamma-Gamma statistics, previous results predict a reduction of fade probability over 80% as a result of introducing the SOA at the receiver [3]. Further, a percentile reduction of the average fade duration of over 85% can be achieved at the SOA output. The authors in [2] derive a mathematical framework that allows for the calculation of Optical Wireless Communication (OWC) link metrics such as the scintillation index and the fade probability for SOA assisted OWC systems operating under weak turbulence. A decrease of 70% - 80% is achieved on the scintillation index at the SOA output [2].

2.2 Spatial Diversity

Another technique for mitigating the effect of turbulence on FSO links is spatial diversity. This involves using multiple apertures at the transmitter and/or receiver so that the inherent redundancy of spatial diversity can significantly enhance performance. Temporal blockage of the laser beam is further reduced and longer distances can be covered even in heavier weather. Figure 2 shows a general spatial diversity system. We consider an FSO system with M transmit apertures and N receive apertures over a discrete-time ergodic channel with Additive White Gaussian noise (AWGN). Binary input, continuous output and intensity modulation, direct detection (IM/DD) with On-Off Keying (OOK) is assumed. The received signal at the nth aperture is given by equation (1) [17]:

$$r_n = x\eta \sum_{m=1}^M I_{mn} + v_n, \quad n = 1, \dots, N \quad (1)$$

where $x \in \{0,1\}$ represents the information bits, η is the optical-to-electrical conversion coefficient, I_{mn} is the irradiance from the mth transmitter to the nth receiver, and v_n is the AWGN with zero mean and variance $\sigma_v = N_0/2$. We assume implicitly that the presence of ambient light in photodetectors can be ignored as a result of Gaussian approximation. Infrared filters can be used over the photodiodes to reduce ambient light in practical

FSO systems. The transmitters and/or receivers are placed a few centimeters (greater than the coherence length) apart to ensure that the received signals are independent of each other.

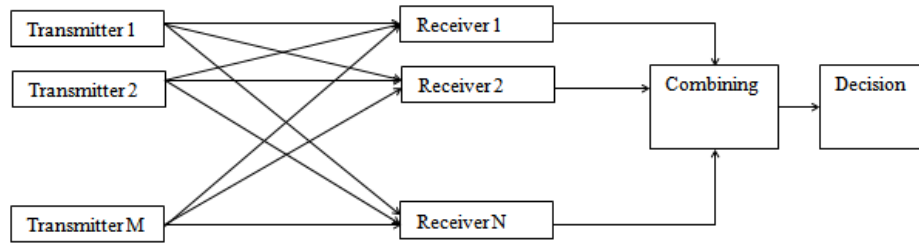


Figure 2: General Spatial Diversity Setup

The first author to propose spatial diversity is [4]. The outage probability of Multiple Input Multiple Output (MIMO) FSO systems over log-normal turbulence channels was investigated by [5][6]. Assuming pulse-position modulation (PPM) [7] and Q-ary PPM [8] both in log-normal and Rayleigh fading regimes, [7] [8] studied MIMO FSO transmissions. In [9], the BER performance of MIMO FSO links for independent and correlated log-normal atmospheric turbulence channels was studied by Navidpour [9].

Spatial Diversity in addition to binary phase shift keying (BPSK)-based subcarrier intensity modulation (SIM) is used to overcome scintillation and avoid the need for adaptive threshold required by optimum on-off-keying (OOK) [22]. SIM is capable of increasing system capacity however at the price of increased signal-to-noise ratio at a particular level of bit-error-rate performance. Equal Gain Combining (EGC) was recommended as it is slightly inferior to maximal ratio combining (MRC) but far less complex to implement.

When using spatial diversity at the receiver side, the three main combining techniques are: Equal Gain Combining (EGC), Selection Combining (SC) and Optimal Combining (OC). At the receiver end, SC techniques select the best signal among all of the signals received from different nodes. Given that each element is an independent sample of the fading process, the element with the highest SNR is selected as shown in equation (2):

$$\begin{aligned} W_k &= 1, & \gamma_k &= \max_n \{\gamma_n\} \\ W_k &= 0, & & \text{otherwise} \end{aligned} \quad (2)$$

Equal gain combining sums all the received signals coherently. In EGC, the weights are varied with respect to the fading signals and the magnitude fluctuates in the order of several 10s of dB. The EGC combiner obviates this problem by setting unit gain at each element. The noise and instantaneous SNR are given by equation (3):

$$P_n = W^H W \sigma^2 = N \sigma^2 \quad (3)$$

The maximal ratio combiner obtains the weights that maximize the output SNR. [6] derived the outage performance of receive diversity systems with SC. They however did not study transmit diversity. In [25], the authors obtained closed-form outage expression for MIMO FSO systems with SC over log-normal turbulence channels. The achievable diversity order was analyzed. Assuming both independent and correlated channels among transmitter/receiver apertures, BER performance of MIMO FSO links over lognormal atmospheric turbulence fading channels was studied in [27]. The effect of diversity in a lognormal channel is different from the Rayleigh fading channel which is usually used to model radio-frequency wireless fading channels.

The authors in [28] investigated the performance of Spatial Mode Multiplexing (SMM) FSO system with mutually coherent channels impaired by both shot noise and thermal noise. An expression was derived for the aggregate achievable rate by describing the detected signal based on a doubly stochastic Poisson model. Also, a mode diversity scheme was proposed and studied in order to enhance the reliability of SMM FSO system in a cost-effective manner.

Atmospheric turbulence and transceiver vibrations are considered in modeling the impairments of terrestrial FSO systems caused by angular fluctuations [29]. The fading induced by angle of arrival fluctuations is modeled accurately by considering atmospheric turbulence and transceiver vibrations. In the thermal and shot noise limited regimes, the outage performance of both coherence and direct detection FSO receiver is analyzed. The benefits of spatial diversity may not be fully achieved when fading among sub-channels is correlated. The authors in [30] studied the average achievable rate (AAR) of spatial diversity MIMO-FSO systems over correlated Gamma-Gamma fading channel under EGC and MRC.

2.3 Aperture Averaging

Aperture averaging is another technique for mitigating scintillation due to atmospheric turbulence. Aperture averaging is the simplest form of spatial diversity where the receiver aperture diameter is made larger

than the coherence length of the atmosphere. The receiver aperture has a finite diameter and the intensity fluctuation is the fluctuation over the whole aperture. The aperture averaging factor is the ratio of the normalized intensity variance measured by a receiver with diameter D to that of a point receiver. The aperture averaging factor is given by equation (4):

$$A = \frac{\sigma_I^2(D)}{\sigma_I^2(D=0)} \quad (4)$$

For plane waves with small inner scale, $l_0 \ll (R/k)^{1/2}$ the aperture averaging factor can be approximated by equation (5):

$$A = \left[1 + 1.07 \left(\frac{kD^2}{4R} \right)^{7/6} \right]^{-1} \quad (5)$$

where D is the receiver diameter, R is the propagation distance, and k is the wave number. The effect of aperture averaging on the received signal can be described by multiplying the scintillation index by the aperture averaging factor.

Using an information theoretic perspective, [23] investigates the combined effects of beamwidth and spatial coherence length on a spatially partially coherent beam (PCB) Gaussian beam. The authors studied the resulting impacts of the optical beam parameters on the average channel capacity of the FSO system in the presence of atmospheric turbulence and pointing errors. Also, the effects of aperture averaging on FSO links using PCBs were considered. In [24], a closed-form analytical expression was derived for the outage probability of a MIMO FSO communication system over Gamma-Gamma turbulence channels. The authors considered the effects of both the inner scale size of optical channel and the aperture averaging.

2.4 Coding Schemes

Channel coding and interleaving can be employed to benefit from some degree of time diversity in free-space optical links. In [32], the authors present a comparative study of the performance of different coding techniques in the presence of channel time diversity. A typical FSO system employing intensity modulation with direct detection (IM/DD) and using On-Off Keying (OOK) modulation was considered. The four channel coding approaches considered are Convolutional Codes, Reed Solomon codes, Concatenated convolutional codes and turbo codes. Convolutional codes generate parity symbols via the sliding application of a Boolean polynomial function to a data stream. Reed-Solomon codes can detect and correct multiple symbol errors. Concatenated codes are obtained by combining an inner code and an outer code. They have both exponentially decreasing error probability with increasing block length and polynomial-time decoding complexity. Turbo codes consist of parallel concatenation of two convolutional codes, with an interleaver between the two codes. Other classes of turbo codes include serial concatenated convolutional codes and repeat-accumulate codes. Convolutional codes are suitable for weak turbulence conditions considering performance improvements and decoding complexity. Under strong turbulence, turbo coding appears to be more appropriate with efficient coding solution. The electrical signal after the optical/electrical conversion is given by equation (6) [32]:

$$r_e = \eta(I_s + I_a) + n \quad (6)$$

where I_s is the received signal light intensity. As shown in equation (7), I_s is equal to the product of I_0 , the emitted light intensity and h , the channel atmospheric turbulence with pdf given [32]:

$$I_s = I_0 h \quad (7)$$

I_a is the ambient light intensity, η is the optical/electrical conversion efficiency, and n is the sum of thermal, dark and shot noise. We assume that I_a is known and can be perfectly cancelled so that the received signal before demodulation is given by equation (8) [32]:

$$r = \eta I_0 h \quad (8)$$

We also assume that $\eta = 1$ and using OOK modulation where presence of I_0 represents symbol $s = 1$ and absences = 0.

$$r = sh + n \quad (9)$$

The maximum a posteriori (MAP) detector gives the detected symbol as shown in equation (10) [32]:

$$\hat{s} = \arg \max_s P(r|s)P(s) \quad (10)$$

To obtain \hat{s} , we assume that n is Gaussian and calculate the logarithmic likelihood ratio (LLR) as shown in equation (11) [32]:

$$LLR = \log \frac{P(r|s=1)}{P(r|s=0)} = \frac{2hr - h^2}{2\sigma_n^2} \quad (11)$$

The symbol is simply obtained by using the sign of the LLRs under hard signal detection. The decision $\hat{s} = 0$ and $\hat{s} = 1$ is made otherwise. Under soft signal detection, the LLR on each transmitted symbol is kept. Soft decoding is performed following soft signal detection except for Reed Solomon code where hard decoding is performed following hard signal detection. The Soft Output Viterbi Algorithm (SOVA) is used for soft input

soft output (SISO) decoding of convolutional codes. We perform outer encoding using Reed Solomon (RS) code followed by outer interleaving and inner convolutional encoding for the concatenated Reed Solomon (CCRS) code. The decoding then consists of SISO decoding of the inner code. This is followed by outer de-interleaving and hard decoding of the outer RS code. The SOVA-based iterative decoding is done for the turbo code.

The authors in [33] studied different scenarios capable of operating under strong atmospheric turbulence and also determined the channel capacity limits. The schemes described for dealing with atmospheric turbulence include: coded-orthogonal frequency division multiplexing (OFDM) scenario, coded-multiple-input-multiple-output (MIMO) scenario and raptor codes based FSO systems. The Low Density Parity Check Code (LDPC) is used in the various scenarios.

An LDPC is a linear error correcting code constructed using a sparse bipartite graph. LDPC are capacity-approaching codes with practical constructions that allow the noise threshold to be set very close to the theoretical maximum for a symmetric memoryless channel. LDPC can be decoded in time linear to their block length using iterative belief propagation. The first approach that can operate in strong turbulence and enable hybrid RF/microwave-optical communication is based on coded-OFDM.

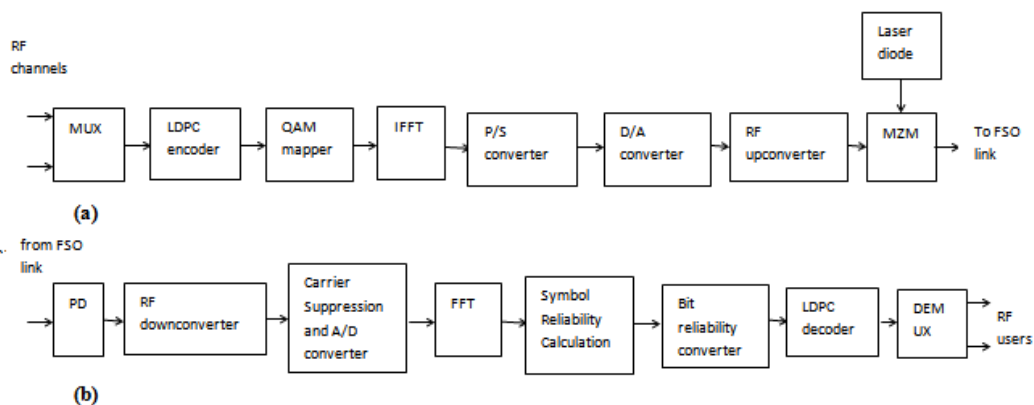


Figure 3: LDPC-coded OFDM system (a) transmitter configuration, and (b) receiver configuration

Figure 3(a) shows the block diagram for the transmitter configuration of LDPC-coded OFDM system while Figure 3(b) shows the receiver configuration. Input data stream from L different RF channels are combined by the multiplexer and encoded using an LDPC encoder. The LDPC encoded stream is separated into groups of B bits. The B bits in each group are subdivided into K subgroups with the i^{th} subgroup containing b_i bits. The b_i bits from the i^{th} subgroup are mapped into a complex-valued signal from a 2^{b_i} -point signal constellation such as QAM. The values of the Discrete Fourier Transform (DFT) of a multicarrier OFDM signal is the complex-valued signal points from all the K subchannels.

The OFDM signal drives the Mach-Zehnder Modulator (MZM) for transmission over the FSO link after D/A conversion and RF up-conversion. An optical system receives the light, and focuses it onto a detector. The transmitted signal is demodulated using the FFT algorithm. This occurs after the RF down-conversion, carrier suppression, A/D conversion and cyclic extension removal. The symbol reliabilities are estimated using the soft outputs of the FFT demodulator. These are then converted to bit reliabilities and used as input to an LDPC iterative decoder.

The coded-MIMO concept is the second approach for communication over strong turbulence channels. Figure 4 shows the coded-MIMO concept with M optical sources all pointed towards the distant array of photodetectors using an expanding telescope. Our assumption is that the beam spots are wide enough to illuminate an entire photodetector array. LDPC encoding is used on the information bearing signal. K encoded bits are sent from the LDPC encoder to the Space Time (ST) encoder. The input bits are mapped into the $T \times M$ matrix using the ST-encoder. The replication of the same one-block ST code over two independent identically distributed blocks is common in schemes that extract spatial and temporal diversity. The one-block Space Time (ST) code can be either a Repetition Code, an Orthogonal Space Time code or a Golden Light code. The author in [34] proposed a replicated coding scheme based on the Golden Light Code (GLC) which can be decoded using Maximum Likelihood decoder. LDPC-coded MIMO can be combined with an appropriate multilevel modulation scheme such as the Q -ary pulse-position modulation (PPM) or Q -ary pulse amplitude modulation (PAM).

Significant improvement over uncoded FSO is achieved using fixed rate error correction codes described as long as temporal correlation can be broken by means of interleavers or a combination of

interleavers and OFDM. The interleaver size can be too large to be practical when the bit duration is short compared to correlation time even if OFDM is used. The use of rate-less codes has been proposed for overcoming this problem. Error-correcting codes such as Raptor codes that adapt to the quality of the channel by varying their user information rate are called rateless codes. As the signal to noise ratio decreases, Raptor codes modify their rate by increasing the codeword length.

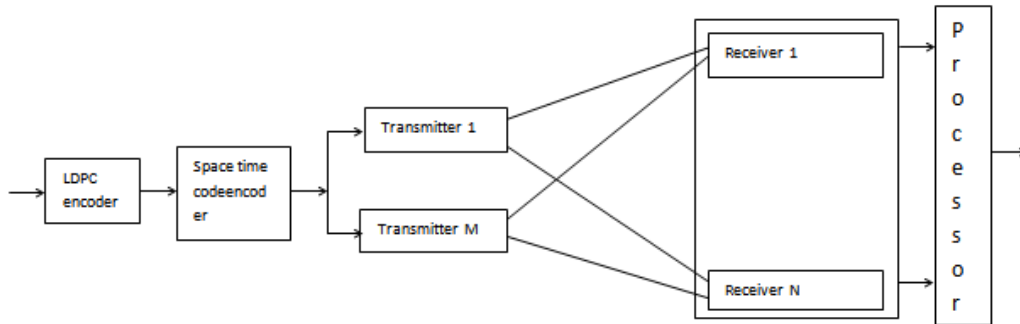


Figure 4: FSO LDPC-coded MIMO system with space-time block codes

III. System And Channel Models

A Free Space Optical (FSO) communication system includes a transmitter, a channel and a receiver. We discuss various models for the transmitter, channel and receiver of an FSO communication system. Further, we discuss relay-assisted FSO systems and far-field assumptions.

3.1 System and Channel Models

A typical FSO system consists of M transmit lasers and N aperture receivers where M, N can be greater than or equal to 1. The FSO system is described as Single-Input-Single-Output (SISO) when M=N=1, Multiple-Input-Single-Output (MISO) when N=1, Single-Input-Multiple-Output (SIMO) when M=1 and Multiple-Input-Multiple-Output (MIMO) when both M and N are greater than 1. On-Off Keying (OOK), Pulse Position Modulation (PPM) and Q-ary PPM have been used as modulation schemes in some previous work because of low cost and simplicity. The binary On-Off Keying (OOK) is described in equation (12):

$$\begin{aligned} s_0(t) &= 0, & 0 \leq t \leq T \\ s_1(t) &= 1, & 0 \leq t \leq T \end{aligned} \quad (12)$$

where T is the symbol duration and the signal set $S = \{s_0, s_1\}$. Some previous work assumed non-ideal photodetector so that thermal and shot noise can be modeled as signal independent Additive White Gaussian Noise (AWGN). FSO systems can be classified as coherent and non-coherent based on detection type. Amplitude, phase and frequency can be used in the coherent receiver system. Non-coherent receiver system uses intensity modulation with direct detection (IM/DD) and there is no need for a local oscillator. IM/DD systems are used in terrestrial FSO systems because of simplicity and low cost. Coherent system provide higher performance in terms of background noise rejection, mitigating turbulent-induced fading, and higher receiver sensitivity.

Various statistical channel models have been proposed to describe weak, moderate and strong atmospheric-induced turbulence fading. Weak atmospheric turbulence is defined as the regime for which the Scintillation Index (SI) is less than 1. The SI parameterizes the scintillation probability distribution function and it is a measure of the strength of fading. The SI is the normalized variance of irradiance fluctuations at the receiving aperture. It is defined in equation (13) [17]:

$$\sigma_I^2 = \frac{E[I^2] - E^2[I]}{E^2[I]} \quad (13)$$

Under weak turbulence, the SI is proportional to the Rytov variance. Under strong turbulence, the SI becomes saturated and it can be much smaller than that predicted by the Rytov Model. The Rytov variance for weak, moderate and strong turbulence respectively are determined as: $\beta_0^2 < 1$, $\beta_0^2 \approx 1$, and $\beta_0^2 \gg 1$ as shown in equation (14):

$$\beta_0^2 = 0.5 C_n^2 k^{7/6} L^{11/6} \quad (14)$$

where $k = 2\pi/\lambda$ is the wave number, λ the wavelength, C_n^2 is the index of refraction structure constant and L is the path length. The log-normal distribution is used to model weak turbulence conditions while the Beckmann distribution, K distribution, and Gamma-Gamma distribution have been proposed to model moderate-to-strong turbulence conditions. The exponential distribution is used to model strong turbulence [31]. In the log normal model, the path gain $A = e^X$ where X is Gaussian distributed with mean μ_X and variance

σ_x^2 . The logarithm of A follows a normal distribution. The probability distribution function of the log-normal model is given in equation (15) [22][31]:

$$f_{I_i}(I) = \frac{1}{(2\pi\sigma_x^2)^{\frac{1}{2}}I} \exp\left(-\frac{(\ln \frac{I}{\bar{I}_i} - \mu_x)^2}{2\sigma_x^2}\right) \quad (15)$$

The Gamma-Gamma distribution models the irradiance of the received optical wave as $I = xy$ where x and y are two statistically independent random processes each of them with a Gamma distribution arising from large and small-scale turbulent eddies. The probability distribution function of the Gamma-Gamma distribution is given in equation (16) [17][31][32]:

$$f_{I_i}(I) = \frac{2(km)^{(k+m)/2} I^{\frac{k+m}{2}-1}}{\Gamma(k)\Gamma(m)\bar{I}_i} K_{k-m}\left(2\sqrt{km\frac{I}{\bar{I}_i}}\right) \quad (16)$$

where $\Gamma(z) = \int_0^\infty e^{-t} t^{z-1} dt$ is the Euler's Gamma function, and $K_v(\cdot)$ is the Bessel function of the second kind and order v . The positive parameters k and m are the effective numbers of respectively large and small-scale turbulent cells. The Gamma-Gamma distribution reduces to the K-distribution in strong fluctuation regime and the system has the same SNR exponent as the exponential case which is used to model very strong fluctuation regimes. The exponential distribution is described in equation (17)[31]:

$$f_{I_i}(I) = \lambda \exp\left(-\lambda \frac{I}{\bar{I}_i}\right) \quad (17)$$

The K distribution has been proposed for strong turbulence [10]. This channel model was used to evaluate the performance of coded FSO systems considering the pairwise error probability and bit error rate (BER) [11]. In [12], the authors extended their results for a correlated K turbulence model where an exponential correlation profile is adopted. The BER performance of a FSO heterodyne system over the K channel was studied in [13]. The performance of single-input single-output (SISO) FSO links suffers from turbulence and requires the use of fading-mitigation techniques such as error control coding in conjunction with interleaving [12][14], and maximum likelihood sequence detection (MLSD)[15]. Also, the performance of MIMO FSO links over independent and not necessarily identically distributed K turbulence channels have been studied [16][17]. A unifying statistical model, the Double Generalized Gamma (Double GG), is proposed in [26]. This proposed unified model remains valid under all range of turbulence conditions (weak to strong) with most of the statistical models for irradiance fluctuations in the literature as special cases. The Gamma-Gamma and Double Weibull models were compared to the proposed model.

3.2 Relay-assisted Free Space Optical Communication Systems

Relay-assisted systems use relays to extend the coverage area of free-space optical communications. The outage probability of amplify and forward (AF) and decode and forward (DF) schemes over strong turbulence channels have been studied [18][19]. Relay-assisted FSO transmission was first proposed in [20]. They can be employed in either in serial (multi-hop transmission) or parallel (cooperative diversity) configurations. In cooperative diversity, the signal transmitted by the source node is heard by the other partner or relay nodes so that the source and partner or relay nodes can jointly process and transmit their information. Multi-hop transmission employs relays in a serial configuration. In figure 5a, the source S transmits an intensity-modulated signal to the relay node R_1 in serial relaying. The relay decodes the signal after direct detection, modulates it and retransmits to the next relay under the decode and forward scheme. The relay multiplies by a proper energy scaling term and forwards to the next relay under the amplify and forward scheme. In the parallel relaying scheme shown in figure 5b, the source node transmits the same signal to N relays. The source has a multi-laser transmitter and each of the lasers point in the direction of a corresponding relay node since broadcasting is not possible due to the nature of FSO communication. [20] is based on a networking perspective while [19] focuses on the physical layer aspects.

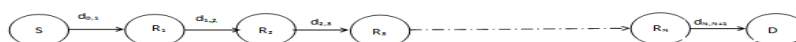


Figure 5a: FSO serial relaying configuration

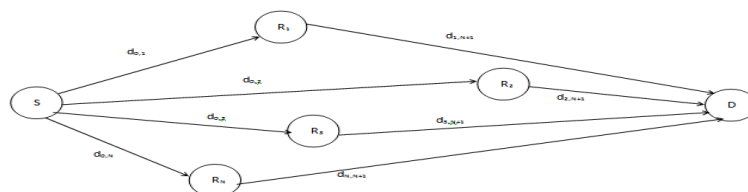


Figure 5b: FSO parallel relaying configuration

There is outage in decode and forward serial relaying scheme whenever there is outage in any of the intermediate SISO links. The outage probability of the end-to-end serial relaying scheme is given by equation (18) [19]:

$$P_{out} = Pr\left(\bigcup_{i=0}^N \{\gamma_i < \gamma_{th}\}\right) \quad (18)$$

$$P_{out} = 1 - Pr\left(\bigcap_{i=0}^N \{\gamma_i > \gamma_{th}\}\right) \quad (19)$$

$$P_{out} = 1 - \prod_{i=0}^N (1 - P_{out,SISO}(d_{i,i+1})) \quad (20)$$

The SNRs of the intermediate SISO channels with lengths $d_{0,1}, d_{1,2}, \dots, d_{N,N+1}$ are $\gamma_1, \gamma_2, \dots, \gamma_N$. There is outage in the decode and forward parallel relaying scheme if either the decoded set D is empty or there is an outage in the MISO (multiple-input single-output) link between the decoding relays and the destination. The decoded set has 2^N possibilities. $S(i)$ is the i^{th} possible set and $Pr(S(i))$ is the probability of the event $\{D=S(i)\}$. For the parallel relaying scheme, the outage probability is given by equation (21) [19]:

$$P_{out} = \sum_{i=1}^{2^N} P_{out,MISO}(\bar{d}_{S(i)}) Pr(S(i)) \quad (21)$$

3.3 Far-field Assumptions

The analytical model of atmospheric turbulence is usually simplified by far field assumptions. In many geometrical scenarios of practical interest, performance analyses show that far field assumption may not correctly estimate system behavior. Diffraction and spatial correlation of atmospheric turbulence degrade system performance, resulting in diversity gain reduction in diversity systems and crosstalk in multiplexing systems.

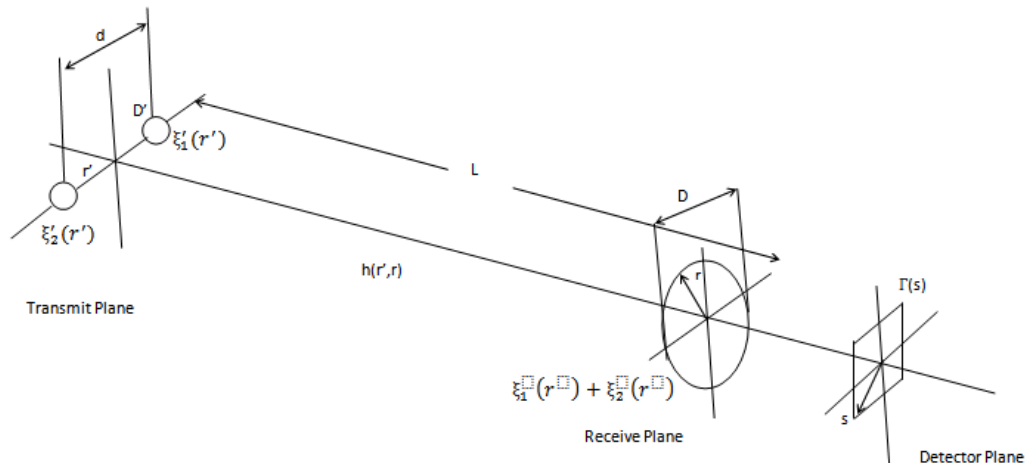


Figure 6: A typical free space optical system with N=2 apertures at the transmitter and a large aperture at the receiver

In [21], the authors consider a more accurate model using near-field assumptions for multi-beam FSO systems. In Figure 6, N=2 laser sources positioned at the transmit plane emit optical beams towards a large aperture positioned at the receiver plane. The optical field received at the large aperture is focused by the receiver lens on the photo-detection area positioned at the detector plane. Multiple transmitters repeat the same signal. The receiver has a single photodetector which converts the total optical power received by the large aperture into electrical signal. By using spatial diversity at the transmitter (multi-beam transmission) and the receiver (large aperture), the reliability of the system is enhanced. Also, the multibeam FSO can be used in multiplexing. Multiple separated transmitters send independent signals and an array of detectors is used at the receiver. The transmitted spatial beam pattern $\xi'_i(r')$ from a circular pupil with diameter D' located at $r' = t_i$ propagates through a path of length L in the atmosphere. It is received within a pupil of diameter D . The received field pattern $\xi_i(r)$ is given by equation (22) [21]:

$$\xi_i(r) = \int \xi'_i(r') h(r', r) e^{-\alpha L/2} dr' \quad (22)$$

$$h(r', r) = \frac{e^{jkL + jk|r-r'|^2/2L}}{j\lambda L} e^{j\chi(r', r) + j\varphi(r', r)} \quad (23)$$

$h(r', r)$ is the paraxial Green's function for atmospheric propagation through clear turbulent air. The stochastic log-amplitude and phase fluctuations caused by atmospheric turbulence is given as $\chi(r', r)$ and $\varphi(r', r)$ respectively. The wavelength is λ . The wave number is k . Analytical characterization of multi-beam FSO systems may not lead to closed form solution without far-field assumptions. In the far-field limit, $L \rightarrow \infty$, $D, D' \rightarrow 0$, $d \rightarrow \infty$. Numerical channel modeling can be performed using the method of random wave vectors (RWV). Also Karhunen-Loeve decomposition or multiple random phase screens can be used although they are not computationally efficient. Samples of log amplitude and phase distortions are obtained and used to evaluate the performance of multi-beam FSO system through Monte Carlo simulation. Practical FSO systems with compact multi-beam transmitter and/or large receive aperture can be designed using the near-field approach.

IV. Conclusions

Free space optical communication has the potential of providing low-cost, license-free, rapidly-deployable and high capacity links. Atmospheric turbulence results in time-varying changes in the refractive-index which further results in time-varying power fluctuations noticeable over distances of 1km or longer. In this paper, we discussed previous work on techniques to mitigate the effects of scintillation on free space optical communication systems. These techniques include equalization in semiconductor optical amplifier, spatial and temporal diversity, aperture averaging and coding schemes. We also reviewed relay-assisted free space optical communication systems and far-field assumptions.

References

- [1]. Mohammad Abtahi, Pascal Lemieux, Walid Mathlouthi and Leslie Ann Rusch, Suppression of Turbulence-Induced Scintillation in Free-Space Optical Communication Systems Using Saturated Optical Amplifiers, *Journal of Lightwave Technology*, volume 24, number 12, 2006.
- [2]. A.C. Boucouvalas, N.C. Sagias and K. Yiannopoulos, First Order Statistics of Semiconductor Optical Amplifier Assisted Optical Wireless Systems under Log-normal Fading, *International Workshop on Optical Wireless Communications*, 2013.
- [3]. Konstantinos Yiannopoulos, Nikos C. Sagias and Anthony C. Boucouvalas, Fade Mitigation Based on Semiconductor Optical Amplifiers, *Journal of Lightwave Technology*, volume 31, number 23, December 2013
- [4]. M.M. Ibrahim and A.M. Ibrahim, "Performance analysis of optical receivers with space diversity reception. *IEEE transactions on wireless communications*, vol. 8, No 2, February 2009
- [5]. E.J. Shin and V.W.S. Chan, "Optical communication over the turbulent atmospheric channel using spatial diversity", in *Proc. IEEE Conf. Global Communication. (GLOBECOM '02)*, Nov. 2002
- [6]. E.J. Shin and V.W.S. Chan, "Part I: optical communication over the clear turbulent atmospheric channel using diversity," *IEEE Journal on Selected Areas in Communication*, vol. 22, no 9, pp. 1896-1906, Nov. 2004
- [7]. S.G. Wilson, M. Brandt-Pearce, Q. Cao, and M. Baedke, "Optical repetition MIMO transmission with multipulse PPM," *IEEE Trans. Journal on Selected Areas in Communication*, vol. 9, no. 23, pp. 1901-1910, Sept 2005
- [8]. S.G. Wilson, M. Brandt-Pearce, Q. Cao, and J.H. Leveque-III, "Free-space optical MIMO transmission with Q-ary PPM", *IEEE Transaction on Communications*, vol. 53, no. 8, pp 1402-1411, Aug. 2005
- [9]. S.M. Navidpour, M. Uysal, and M. Kavehrad, "BER performance of free-space optical transmission with spatial diversity," *IEEE Trans. On Wireless Communication*, vol. 6, no 8, pp. 2813-2819, Aug 2007
- [10]. E. Jakeman and P.N. Pusey, "A model for non-Rayleigh sea echo", *IEE Transaction of Antennas and Propagation*, vol. 24, pp 806 – 814, Nov 1976.
- [11]. M. Uysal and J.T. Li, "BER performance of coded free-space optical links over turbulence channels," in *Proc. IEEE Vehicular Technology Conference (VTC Spring)*, Milan, Italy, May 2004, pp. 168-172
- [12]. M. Uysal, S.M. Navidpour and J.T. Li, "Error rate performance of coded free-space optical links over strong turbulence channels", *IEEE Communication Letters*, vol. 8, pp 635-637, Oct 2004
- [13]. K. Kiasaleh, "Performance of coherent DPSK free-space optical communication systems in K-distributed turbulence," *IEEE transaction on communications*, vol. 54, no 4 pp. 604 – 607, April 2006
- [14]. X. Zhu and J.M. Kahn, "Performance bounds for coded free-space optical communications through atmospheric turbulence channels," *IEEE transaction on communications*, vol 51, pp 1233-1239, August 2003
- [15]. X. Zhu and J.M. Kahn, "Markov chain model in maximum-likelihood sequence detection for free space optical communication through atmospheric turbulence channels," *IEEE Transaction of Communication*, no 3, 2003
- [16]. Theodoros A. Tsiftsis, Harilaos G. Sandalidis, George K. Karagiannidis and Murat Uysal, FSO links with spatial diversity over strong atmospheric turbulence channels, *Proceedings of IEEE Communications Society, ICC 2008*
- [17]. Theodoros A. Tsiftsis, Harilaos G. Sandalidis, George K. Karagiannidis and Murat Uysal, Optical Wireless Links with spatial diversity over strong atmospheric turbulence channels, *IEEE transactions on wireless communications*, vol. 8, no. 2, February 2009.
- [18]. Theodoros A. Tsiftsis, Harilaos G. Sandalidis, George K. Karagiannidis and Nikos C. Sagias, "Multihop free-space optical communications over strong turbulence channels, *Proceedings of IEEE ICC 2006*
- [19]. Majid Safari and Murat Uysal, Relay-assisted free-space optical communication, *IEEE transactions on wireless communications*, vol 7, no 12, December 2008
- [20]. A.S. Acampora and S.V. Krishnamurthy, "A broadband wireless access network based on mesh-connected free-space optical links," *IEEE Personal Communications*, vol 6, pp 62-65, October 1999
- [21]. Majid Safari and Steve Hranilovic, Diversity and multiplexing for near-field atmospheric optical communication, *IEEE Transactions on Communications*, vol 61, No 5, May 2013
- [22]. W.O. Popoola, Z. Ghassemlooy, J.J.H. Allen, E. Leitgeb and S. Gao, Free-Space optical communication employing subcarrier modulation and spatial diversity in atmospheric turbulence, *IET Optoelectronics*, 2008, vol 2, no 1, pp 16-23

- [23]. It Ee Lee, ZabihGhassemlooy, Wai Pang Ng, Mohammad-Ali Khalighi and Murat Uysal, Capacity analysis of free-space optical links for a partially coherent Gaussian beam over a turbulent channel with pointing errors, 18th European conference on Network and Optical Communications and 8th Conference on optical cabling and infrastructure, July 2013
- [24]. HosseinKazemi, ZohrehMostaani, Murat Uysal, and ZabihGhassemlooy, Outage Performance of MIMO Free-space optical systems in Gamma-Gamma fading channels, 18th European conference on Network and Optical Communications and 8th Conference on optical cabling and infrastructure, July 2013
- [25]. HosseinKazemi and Murat Uysal, Performance analysis of MIMO free-space optical communication systems with selection combining, 21st Signal Processing and Communications Applications Conference, April 2013
- [26]. Mohammadreza A Kashani, Murat Uysal and Mohsen Kavehrad, A novel statistical model for turbulence-induced fading in free-space optical systems, 15th International Conference on Transparent Optical Networks, ICTON, June 2013
- [27]. S. Mohammad Navidpour, Murat Uysal and Jing (Tiffany) Li, BER performance of MIMO free-space optical links, 60th IEEE Vehicular Technology Conference, September 2004
- [28]. Huang, S, RaoofMehrpoor, G & Safari, M, 'Spatial-Mode Diversity and Multiplexing for FSO Communication with Direct Detection' IEEE Transactions on Communications, 2018
- [29]. Huang, S & Safari, M, 'Free-Space Optical Communication Impaired by Angular Fluctuations' IEEE Transactions on Wireless Communications, 2017
- [30]. Thanh V. Pham, Truong C. Thang, &Anh T. Pham, Average Achievable Rate of Spatial Diversity MIMO-FSO Over Correlated Gamma-Gamma Fading Channels, Journal of Optical Communication Networks, vol. 10, No 8, August 2018
- [31]. Nick Letzepis, Albert Guillen I Fabregas, Outage Probability of the MIMO Gaussian Free-Space Optical Channel with PPM, ISIT 2008, July 2008
- [32]. Fang Xu, Mohammad-Ali Khalighi, Patrice Causse and Salah Bourenname, Performance of Coded Time-Diversity Free Space Optical Links, 24th Biennial Symposium on Communications, 2008
- [33]. Ivan B. Djordjevic, Coding For Free Space Optical Communication , 21st Annual Meeting of the IEEE Lasers and Electro-Optics Society, Nov, 2008
- [34]. LinaMroueh, Extended Golden Light Code for FSO-MIMO Communications with Time Diversity, IEEE Transactions on Communications, 2018